Proceedings of Ninth World Conference on Earthquake Engineering
August 2-9, 1988, Tokyo-Kyoto, JAPAN (Vol.II)

3-6-1

PREDICTION OF HIGH-FREQUENCY STRONG MOTIONS BASED ON HETEROGENEOUS FAULTING MODEL

Tomotaka Iwata and Kojiro Irikura

Disaster Prevention Research Institute, Kyoto University,

Gokasho, Uji-shi, Kyoto, 611, Japan

SUMMARY

A synthesis procedure is presented to predict the high-frequency strong ground motion produced by a faulting model. We developed an inverse Radon-transform method to recover the distribution of maximum slip velocity on the fault by using near-field seismograms. Our approach combines back-projection with a windowing procedure. This method is suited for scarce and non-uniform observation points.

Next, based on this slip velocity distribution, we synthesized near-field acceleration seismograms using the records from small event as an empirical Green's function. We get a successful prediction of high-frequency strong motions by using a heterogeneous faulting model for large earthquake.

INTRODUCTION

One of the goals of engineering seismology is to predict high-frequency ground motions given certain characteristics of faulting. It is accepted that high-frequency ground motions may be induced by the heterogeneities of the rupture. For example, we can consider variations of stress drop (asperity model, Ref.1) or an irregular rupture velocity distribution (barrier model, Ref.2). The assessment of the effects of these heterogeneities on rupture propagation during large earthquakes is a key issue in predicting strong ground motions.

In this paper, we consider two main subjects. First, using the acceleration records observed at several stations, we estimate the areas generating high-frequency seismic waves on the fault plane of a large earthquake. We developed an inverse Radon-transform method to recover maximum slip velocity on the fault plane. Second, based on the inferred slip velocity distribution, we synthesize near-field acceleration seismograms for the large shock using the records from one small event as an empirical Green's function and compare the synthetic waveforms with the observed ones. We also discuss the differences between the synthetics for the uniform slip faulting model and those for the heterogeneous faulting model.

INVERSION PROCEDURE

The far-field ground displacement $\mathbf{U}(\mathbf{x},t)$ is described by

$$U(x,t)=\int_{\Sigma}\Delta\dot{u}(\xi,t)*G(\xi;x,t)d\xi \qquad (1)$$

(Ref.3) where $\Delta\dot{u}(\xi,t)$ is slip velocity function, $G(\xi;x,t)$ is the Green's function from the point ξ on the fault plane Σ to the observation point x and * denotes convolution. We choose slip functions of the form

$$\Delta \dot{u}(\xi,t)=f(t-t_r(\xi))K(\xi) \qquad (2)$$

where we say point ξ ruptures at time $t_r(\xi)$ and the amplitude of rupture $K(\xi)$ is assumed to be a function of position only. The time function $f(t-t_r(\xi))$ was obtained by Day (Ref.4) in spontaneous rupture models. We show a sketch of the slip velocity time function in Fig.1(a). Considering the contribution for high-frequency radiation, we can approximate this slip velocity function by delta-like-function $\Delta\dot{u}_{max}\delta(t-t_r(\xi))$ (Fig.1(b)). If we deconvolve the observed seismogram with the path effect by some adequate method, we can estimate the source time function $S(x,t)$. This source time function is approximated to the integration of maximum slip velocity along the isochrone(Ref.5), which depends on the fault-observation point geometry, wave velocity, and rupture velocity,

$$S(x,t)=\int_{l=l(x,\xi)} \Delta \dot{u}_{max}(l)dl \qquad (3).$$

This formula is the Radon-transform. For inverting the transform (3), we use the back-projection method with a windowing procedure. This method is suited for scarce and non-uniform observation points. We show this procedure applied to a model simulation in the case of the fault-observation point geometry for the 1980 Izu-Hanto-Toho-Oki earthquake (M_{JMA}=6.7). Fig. 2 shows the map of locations of the observation stations (triangles), the hypocenter (closed square), and the inferred fault plane of 1980 Izu-Hanto-Toho-Oki earthquake.

In Fig. 3, we show the flow-chart of the reconstruction method. A simple example of the source process recovering is displayed for an asperity model(Ref.1) in which non-zero slip velocity function exists at two pixels on the fault plane. The result of the windowed back-projection reconstruction (Fig.3(f)) recover well the model of the distribution of slip velocity (Fig.3(a)). Applying this procedure to our data set, we can estimate the distribution of maximum slip velocity (MSV) on the fault plane.

ESTIMATION OF THE DISTRIBUTION OF MAXIMUM SLIP VELOCITY

In order to estimate the source time function $S(x,t)$ at each station for the inverse procedure, we eliminated the path effect from observed seismograms using the records from a small event as an empirical Green's function with the Winner filtering technique. In Fig.4, we show an example of the seismic traces and the design of the Wiener filter (Fig.4(c)) for predicting the source time function. The filter coefficient series obtained above correspond to the source time function. Generally, the source time function may be a positive-value function with the positive slip velocity. However, the filter coefficient series are not a positive function. This is caused by a random error in the deconvolution process. The filter coefficient can be expressed in terms of a time-dependent amplitude (envelope) and a time-dependent phase. In the high frequency range, the time-dependent phase is not reliable. We assume that the envelope of the filter coefficient series represent the source time function. The envelope of the filter coefficient series (Fig.4(e)) are smoothed by a bell-shaped time window to account for the finite source duration of the small event. Fig.4(f) regards to the source time function at KWN.

Using the source time functions which correspond to the 5 stations, we recover the distribution of MSV on the fault plane which appears in Fig. 5(b). The rectangle with bold lines shows the fault plane. "H" indicates high MSV. The MSV with larger amplitudes appear in the northern part of the fault plane. This result suggests that the rupture process in the north part of the fault plane gives the most significant contributions to the high-frequency radiation. Fig.5(a) displays the epicentral distribution of the 1980 Izu-Hanto-Toho-Oki earthquake and its aftershocks(M>2.9), which were observed within 10-hours after mainshock occurrence (Ref.6,Fig.11). The area in which high maximum slip velocity was generated corresponds to the zone with less aftershock occurrence.

SYNTHESIS OF HIGH-FREQUENCY STRONG MOTIONS BASED ON HETEROGENEOUS FAULTING MODEL

Based on the heterogeneous slip velocity distribution obtained above, we synthesize near-field acceleration seismograms using the records from a small event as an empirical Green's function(Ref.7). The synthetic result is illustrated for the mainshock accelerations at KWN, the nearest observation station from the hypocenter.

The observed accelerogram from the mainshock at KWN and the synthetic seismograms are illustrated in Fig.6. The envelope of the synthesized waveforms for heterogeneous fault model agrees better with the observed ones than those for the uniform slip model.

CONCLUSIONS

We propose an inverse Radon-transform method to reconstruct the distribution of maximum slip velocity on the fault plane of a large earthquake by using near-field seismograms. The obtained maximum slip velocity distribution for the 1980 Izu-Hanto-Toho-Oki earthquake is heterogeneous on the fault plane. Based on this slip velocity distribution, we synthesized near-field acceleration seismograms using the records from small event as an empirical Green's function. Successful prediction of high-frequency strong motions were obtained by using a heterogeneous faulting model for the large earthquake.

ACKNOWLEDGMENTS

We would like to thank K. Kudo of Earthquake Research Institute, University of Tokyo and K. Ishida of Center Research Institute of Electric Power Industry, Japan for providing the digital accelerograms.

Fig.1

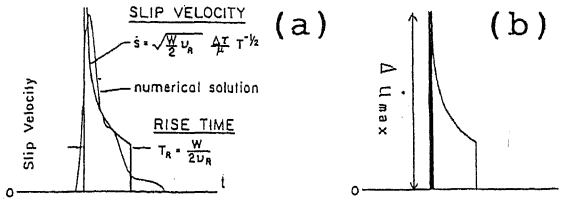

Fig. 1 (a): Sketch of the slip velocity time function obtained by Day(Ref.4, Fig.14). The thin line shows the numerical solution with spontaneous rupture propagation and the thick line shows the approximated time function. (b): Approximated slip velocity time function for high-frequency asymptote. The thick line shows the same as (a). The bold line shows the maximum slip velocity time function assumed in this study.

Fig.2

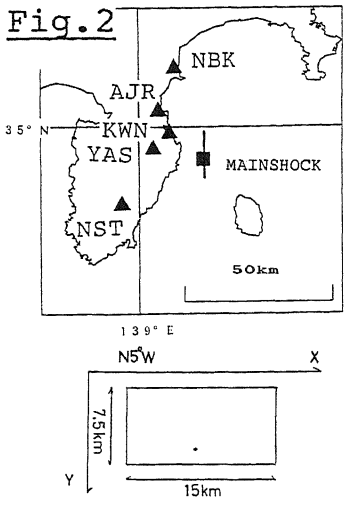

Fig. 2 The map of observation station (triangle) and location of the hypocenter (closed square), and the inferred fault plane of 1980 Izu-Hanto-Toho-Oki earthquake.

Fig. 3 (a): The distribution of slip velocity function is displayed for an asperity model in which non-zero slip velocity function exists at two pixels on the fault plane. In our bird-eye's pictures, X- and Y-axes correspond to north and south, bottom and top, respectively. In this case, the rupture smoothly propagates from the center (indicated by an arrow) with constant rupture velocity of 3.0km/s. (b): The envelopes of the calculated waveforms from the given distribution of slip velocity are shown. Top and bottom traces correspond to the source time functions at NBK and KWN, respectively. (c): The back-projection reconstructions into the fault plane of source time function at NBK and KWN, respectively are displayed. (d): The sum of the back-projection reconstructions using the source time functions at 5 stations. This figure does not reproduce well the given slip velocity distribution. (e): A windowing procedure scheme. The isochrone form depends on the geometrical relation between the station and the fault plane configuration, wave velocity and rupture velocity. For each station, we search the pixels on the fault plane, through which the isochrone with the time corresponding to the non-zero value source-time function passes. We give flags to those pixels. Then we get a flag map on the fault plane for each station. We take a logical product between those flag maps, then we find the (discrete) spatial window function [W(x,y)] of the fault plane. (f): The back-projection reconstruction for each station is windowed by W(x,y). The bottom figure shows the sum of windowed back-projection reconstruction. This reconstruction result recovers well the original distribution of slip velocity.

Fig.3

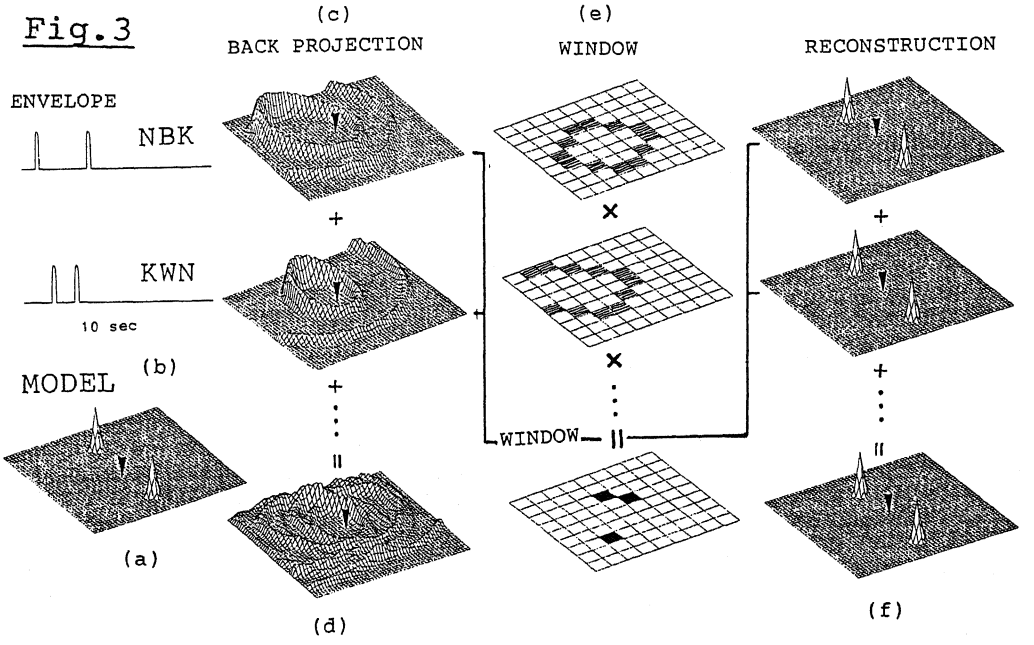

Fig.4

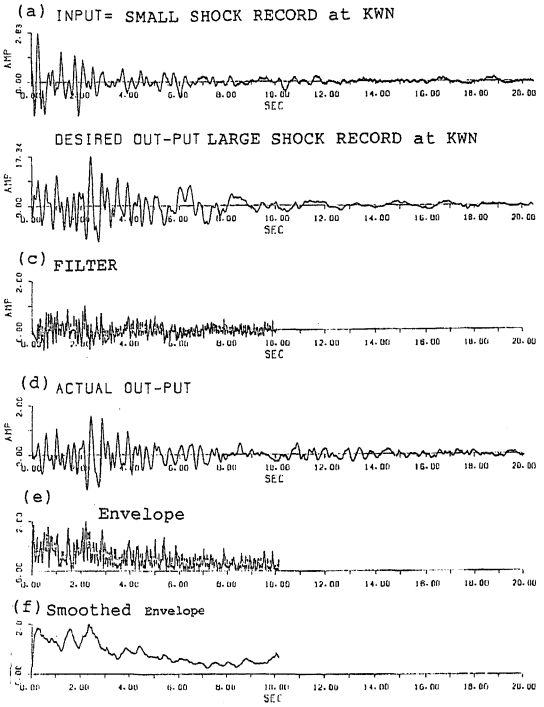

Fig.5

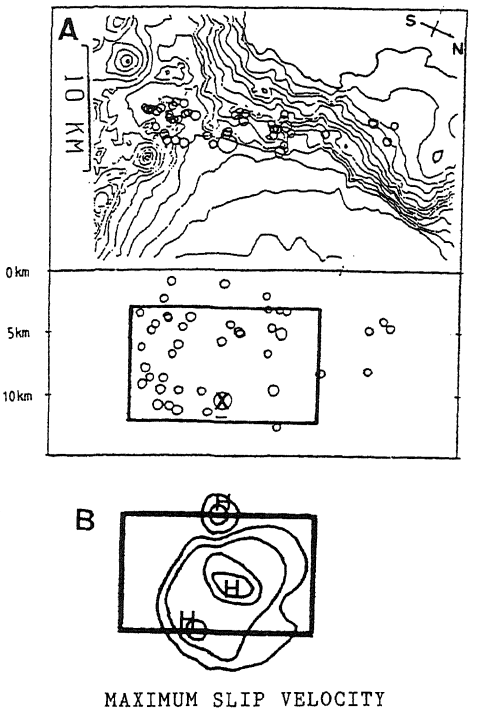

Fig. 4 (a): The accelerogram of the small aftershock (M_{JMA}=4.9) recorded at KWN. The trace shows the NS component record from the onset of S-waves. The record is added with noise with zero-mean and 1% standard deviation of the maximum signal amplitude for stabilizing the solution. (b): The accelerogram of the mainshock recorded at KWN. The trace also shows the NS component record from the onset of S-waves. This trace is the desired output for the filtering. (c): The estimated filter coefficient series. (d): The actual output series for this deconvolution. (e): The envelope of the filter coefficient series (Fig.4(c)). This envelope is smoothed by a bell-shaped time window to account for the finite source duration of the small event. (f) shows the inferred source time function at KWN.

Fig.5 (a): The epicentral distribution of the 1980 Izu-Hanto-Toho-Oki earthquake and its aftershocks(M>2.9). The aftershocks were observed within 10-hours after mainshock occurrence obtained by Matsu'ura(Ref.6,Fig.11). The bottom vertical section is perpendicular to the direction N20°W. The cross indicates the hypocenter of the mainshock. The rectangle shows the inferred fault plane. (b): The contour map of the distribution of maximum slip velocity (MSV) obtained from our reconstruction method. The rectangle with bold lines shows the fault plane same as in (a). "H" indicates high MSV.

Fig.6

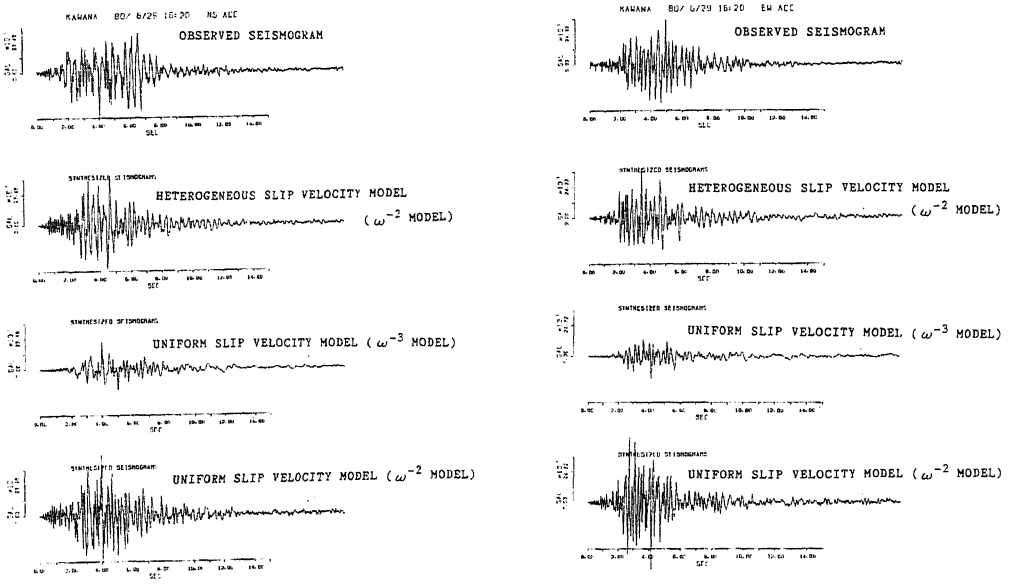

Fig. 6 The observed accelerogram from the mainshock at KWN and the synthetic seismograms. The left panel shows the NS-component and the right panel, the EW-component. From top to bottom, the observed accelerograms, the synthetic seismograms with the heterogeneous slip velocity distribution obtained in this study, with the constraint ω^{-2} model, those with uniform slip velocity distribution based on the ω^{-2} model and those on the ω^{-3} model are displayed.

REFERENCES

1. Lay, T. and H. Kanamori, An asperity model of great earthquake sequences, Earthquake Prediction -An International Review-, Maurice Ewing Series, 4,579-592,(1981)
2. Das, S. and K. Aki, Fault plane with barriers: A versatile earthquake model, J. Geophys. Res., 82, 5658-5670,(1977).
3. Aki, K. and P.G. Richards, Quantitative Seismology: Theory and Methods,W.H.Freeman, San Francisco, California.,(1980)
4. Day, S.M.,Three-dimensional finite difference simulation of fault dynamics:Rectangular faults with fixed rupture velocity ,Bull. Seism. Soc. Am., 72,705-727,(1982)
5. Bernard, P. and R. Madariaga, A new asymptotic method for the modeling of near field accelerograms, Bull.Seism. Soc. Am., 74, 539-558,(1984)
6. Matsu'ura, S.R., Detailed study of the earthquake sequence in 1980 off the east coast of Izu Peninsula, Japan, J. Phys. Earth, 31, 65-101,(1983)
7. Irikura, K., Prediction of strong acceleration motions using empirical Green's function., Proc. 7th Japan Earthquake Engineering, 151-156,(1986)